Electronic population effect in halogen nuclear spin - lattice relaxation in praseodymium trihalide compounds

1996 J. Phys.: Condens. Matter 8 8001

(http://iopscience.iop.org/0953-8984/8/42/018)

J. Phys.: Condens. Matter **8** (1996) 8001–8009. Printed in the UK

Electronic population effect in halogen nuclear spin–lattice relaxation in praseodymium trihalide compounds

Sunyu Su†, Pablo Prado†, Robin L Armstrong† and Mariano Zuriaga‡

† Department of Physics, University of New Brunswick, Fredericton, New Brunswick, E3B 5A3 Canada

‡ Facultad de Matematica, Astronomia y Fisica, Universidad Nacional de Córdoba, 5000 Cordóba, Argentina

Received 28 February 1996

Abstract. Nuclear quadrupole resonance determinations of the spin–lattice relaxation rates of the ^{35}Cl, ^{79}Br and ^{81}Br nuclei in the praseodymium trihalide crystals $PrCl_3$ and $PrBr_3$ are reported. Data are presented in the temperature range 7–297 K. They are shown to be dominated by magnetic dipole interactions between the halogen nuclear spins and the Pr^{3+} paramagnetic ions. The relaxation rates display unusual temperature dependences. This behaviour is a consequence of the crystalline electric field splitting of the ground-state multiplet of the Pr^{3+} configuration into six states, and the resultant depopulation of the ground paramagnetic state as the temperature is raised. The qualitatively different temperature variation for the two compounds is a result of the different energy splittings of the multiplet levels in the two instances. The analysis utilizes an electron-spin correlation time described by a temperature-independent term, the characteristic time for spin exchange between neighbouring ions, plus a temperature-dependent exponential term.

1. Introduction

The praseodymium trihalide compounds $PrCl_3$ and $PrBr_3$ crystallize in the same hexagonal structure. The Pr ion site symmetry is C_{3h} and hence the crystalline electric field (CEF) splits the ground-state multiple $^3H_4$ of the Pr^{3+} $4f^2$ configuration into three doublets ($2\Gamma_5$ and Γ_6) and three singlets (Γ_1, Γ_3 and Γ_4). However, the actual energy splittings of the CEF levels in $PrCl_3$ and $PrBr_3$ are considerably different (Schmid *et al* 1987).

The low-temperature properties of $PrCl_3$, and to a lesser degree those of $PrBr_3$, have been the subject of numerous investigations (Colwell *et al* 1969, Harrison *et al* 1976, Su *et al* 1991, Su and Armstrong 1993). Below 1 K, one-dimensional (1D) magnetic ordering occurs; this is followed by a phase transition at 0.4 K. The 1D behaviour is well described by an effective 1D *XY* Hamiltonian (Harrison *et al* 1976, Goovaerts *et al* 1984). Nuclear quadrupole resonance (NQR) measurements of the halogen spin–lattice relaxation times have been shown to agree with the predictions from relaxation theory for a magnetic dipole interaction (Su *et al* 1991). The phase transition is assumed to be a co-operative Jahn–Teller transition to a three-dimensional (3D) antiferroelectric ordered state; Peierls dimerization has been predicted (Morra *et al* 1983).

Halogen nuclear spin–lattice relaxation times T_1 above 4 K have not been previously reported for either $PrCl_3$ or $PrBr_3$. Such measurements are also expected to be dominated

0953-8984/96/428001+09$19.50

by the magnetic dipole coupling between the paramagnetic ions and the halogen nuclei and hence will provide information on the fast paramagnetic-ion spin dynamics (Birkeland and Svare 1978, Rager 1981, 1984). Mizuno *et al* (1991) have compared the NQR technique with the EPR method, using measurements in $[Co(H_2O)_6][PtCl_6]$, as a means to study electron spin dynamics.

The theory of nuclear-spin relaxation in paramagnetic materials has been discussed for the Zeeman case by Solomon (1955), Bloembergen (1957) and Bloembergen and Morgan (1961). However, this theory has a fundamental limitation in that it assumes that the electron-spin Hamiltonian is the electronic Zeeman Hamiltonian. As a result, the effects of zero-field splitting (ZFS) are neglected except as a mechanism for electron-spin relaxation.

A theory of nuclear-spin relaxation in paramagnetic solutions in the ZFS limit has been developed by Sharp (1990, 1993) and Bovet and Sharp (1993) and for arbitrary Zeeman and ZFS contributions by Sharp (1992).

A theoretical expression for the halide T_1 in PrX_3 as measured in an NQR experiment is derived in section 2. Experimental considerations are presented in section 3. Section 4 contains the results and their interpretation. Section 5 is the conclusion.

2. Theory

The spin–lattice relaxation rate for the halogen nuclei is modelled assuming a magnetic dipole interaction between the halogen nuclear spins ($I = 3/2$) and the electron spins S belonging to the Pr^{3+} ions. For an NQR experiment the nuclear spins are quantized along the direction of the electric field gradient (EFG) generated by the surrounding charges, and the Pr^{3+} electron spins by the molecular field. Taking account of the crystal symmetry and the magnitude of the interacting forces, the EFG tensor can be calculated at the nuclear site. Using the known geometrical parameters and electronic state information (Schmid *et al* 1987) the equations derived can be evaluated.

For nuclei with spin 3/2 the spin–lattice relaxation rate T_1^{-1} can be written as

$$T_1^{-1} = 2W_1 \tag{1}$$

where W_1 is the transition probability corresponding to the transitions $|1/2\rangle \rightleftharpoons |3/2\rangle$ or $|-1/2\rangle \rightleftharpoons |-3/2\rangle$. Using Abragam's (1961) notation we can write the magnetic dipole interaction Hamiltonian in the form

$$\mathcal{H}_1 = \sum_{(q)} F^{(q)} A^{(q)}. \tag{2}$$

It follows that

$$W_1 = 3\alpha^2\hbar^2 \int \langle a_-(0)a_+(\tau)\rangle \exp(-\mathrm{i}\omega_q\tau)\,\mathrm{d}\tau \tag{3}$$

where $\alpha = (3/2)\gamma_I\gamma_S$ with γ_I and γ_S the gyromagnetic ratios of the resonant nuclear spin and praseodymium electron spin, respectively, and ω_q is the NQR frequency. Also

$$a_+(\tau) = F^{(1)}(\tau)S_0(\tau) + (1/6)F^{(0)}(\tau)S_-(\tau) + (1/2)F^{(2)}(\tau)S_+(\tau)$$
$$a_-(\tau) = a_+^+(\tau)$$

where the functions $F^{(p)}(\tau)$ with $p = 0, 1, 2$ are as given by Abragam (1961). Following the procedure of Sharp (1992), but using the nuclear eigenstates determined by the quadrupole

coupling, we obtain

$$\begin{aligned}\langle a_-(0)a_+(\tau)\rangle &= |F^{(1)}(0)|^2 \exp(-\tau/\tau_R)\,\langle S_0(\tau)S_0(0) + (1/6)^2| \\ &\times F^{(0)}(0)|^2 \exp(-\tau/\tau_R)\,\langle S_+(\tau)S_-(0)\rangle + (1/2)^2| \\ &\times F^{(2)}(0)|^2 \exp(-\tau/\tau_R)\langle S_-(\tau)S_+(0)\rangle \end{aligned} \tag{4}$$

where τ_R characterizes the time scale of the molecular motion. The functions $\langle S_p(\tau)S_{-p}(0)\rangle$ with $p = 0, \pm$ are given by

$$\begin{aligned}\langle S_p(\tau)S_{-p}(0)\rangle &= \mathrm{Tr}\{\rho S_p(\tau)S_{-p}(0)\} \\ &= \sum_{\mu\nu} \rho_\mu \langle \Gamma_\mu|S_p|\Gamma_\nu\rangle\langle\Gamma_\nu 0|S_{-p}|\Gamma_\mu\rangle \exp\left(\frac{-\tau}{\tau_{\mu\nu}}\right) \exp[\mathrm{i}(\omega_\mu - \omega_\nu)\tau] \end{aligned} \tag{5}$$

where the ρ_μ are the thermal equilibrium populations of the electronic levels and the $\tau_{\mu\nu}$ are the electron-spin correlation times. Note the difference between this result and the previous result (Mizuno *et al* 1990) where the spin system had no definite axis of quantization.

The main contribution to T_1^{-1} is given by the first term in equation (4); the other terms become small as a result of performing the integration in equation (3). Since $\omega_{\mu\nu} \gg \omega_q$, with μ and ν indicating different electronic energy levels, the transverse components may be neglected. Therefore, T_1^{-1} can be calculated by considering only the term

$$\langle S_0(\tau)S_0(0)\rangle = \sum_\mu \rho_\mu |\langle\Gamma_\mu|S_0|\Gamma_\mu\rangle|^2 \exp\left(-\frac{\tau}{\tau_\mu}\right). \tag{6}$$

Substituting equation (6) in equation (4) gives

$$\langle a(0)a_+(\tau)\rangle = |F^{(1)}|^2 \sum_\mu \rho_\mu |\langle\Gamma_\mu|S_0|\Gamma_\mu\rangle|^2 \exp\left(-\frac{\tau}{\tau_\mu}\right) \tag{7}$$

where we have used the slow molecular motion approximation (Sharp 1992), namely $1/\tau_\mu + 1/\tau_R \approx 1/\tau_\mu$. After performing the integration in equation (3) we obtain

$$T_1^{-1} = A^2 \sum_\mu \rho_\mu |\langle\Gamma_\mu|S_0|\Gamma_\mu\rangle|^2 \left(\frac{\tau_\mu}{1+\omega_q^2\tau_\mu^2}\right) \tag{8}$$

where $A^2 = 6\alpha^2\hbar^2|F^{(1)}|^2$ and $|F^{(1)}|^2 = (1/r^6)\sin^2\theta\cos^2\theta$ with r the distance from the paramagnetic ion to the resonant nucleus, and θ the angle between the principal axis of the EFG and the vector $\boldsymbol{r}$. This equation can be simplified if $\omega_q\tau_\mu \ll 1$, as is usually the case, to yield

$$T_1^{-1} = A^2 \sum_\mu \rho_\mu |\langle\Gamma_\mu|S_0|\Gamma_\mu\rangle|^2 \tau_\mu. \tag{9}$$

The geometrical factor $F^{(1)}$ can be obtained from the Euler angles calculated by the diagonalization of the EFG. The electron spin correlation time may be represented as (Birkeland and Svare 1978)

$$1/\tau_\mu = 1/\tau_S + 1/T_{1\mu} \tag{10}$$

where τ_S is the temperature-independent characteristic time for a spin flip between neighbouring electrons, and $T_{1\mu}$ is the electron spin–lattice relaxation time. This latter quantity will, in the present case, exhibit a complicated temperature dependence as the range of temperatures studied spans all six low-lying electronic energy levels of $PrCl_3$ and $PrBr_3$. An empirical expression for $T_{1\mu}$, namely $T_{1\mu} = T_{\mu 0}\exp(\Delta_\mu/kT)$, was used; Δ may be thought of as a generalized Orbach process energy gap.

3. Experimental details

Halide NQR measurements on polycrystalline samples of $PrCl_3$ and $PrBr_3$ were carried out in the temperature range 7–297 K. The samples were obtained from Dr D R Taylor, Queens University, Kingston, Canada. Temperature control was achieved with a Lakeshore cryogenic controller (TGC-100) in conjunction with a calibrated DT-470-SD-12A silicon diode sensor. In the range 7–77 K the temperature was determined by this sensor; above 77 K a copper–constantan thermocouple was used. Temperature measurements were accurate to within ± 0.5 K.

^{35}Cl, ^{79}Br and ^{81}Br spin–lattice relaxation measurements were obtained using a conventional Fourier transform (FT) NMR spectrometer equipped with a TecMag pulse programmer and acquisition system. The RF pulses were produced by gating the output of a Fluke 616B synthesizer. A π–τ–$\pi/2$ inversion recovery pulse sequence was used. The magnetization recovery was well represented by a single-exponential decay for all temperatures in both compounds. The estimated error in the T_1^{-1}-values obtained from the decay curves is $\pm 3\%$.

The data are shown in figures 1 and 2.

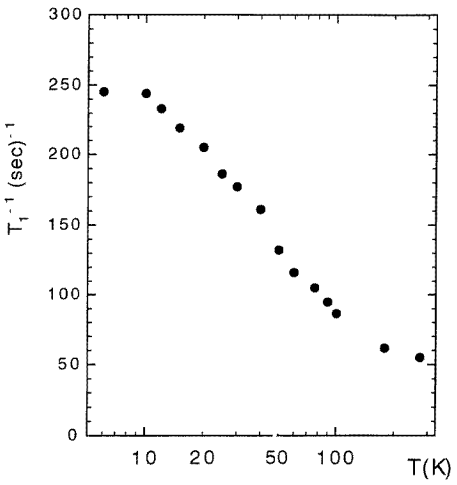

Figure 1. Measured ^{35}Cl relaxation rate data as a function of temperature.

4. Results and discussion

Figure 3 is a plot of the ratio $T_1^{-1}(^{81}\mathrm{Br})/T_1^{-1}(^{79}\mathrm{Br})$ as a function of temperature. The average value of this ratio is 1.17 ± 0.04; the ratio of magnetic dipole moments of the two bromine isotopes is 1.16, as shown by the broken line. This result demonstrates that the relaxation is dominated by the magnetic dipole coupling between the bromine nuclei and the paramagnetic Pr^{3+} ions and not by the electric quadrupole interaction. If the latter mechanism were dominant, the ^{81}Br data would lie below the ^{79}Br data. It is reasonable to assume that magnetic dipole coupling also dominates the relaxation for $PrCl_3$.

From figures 1 and 2 we see that the temperature dependences of T_1^{-1} for $PrCl_3$ and $PrBr_3$ are qualitatively different at the higher temperatures even though both compounds

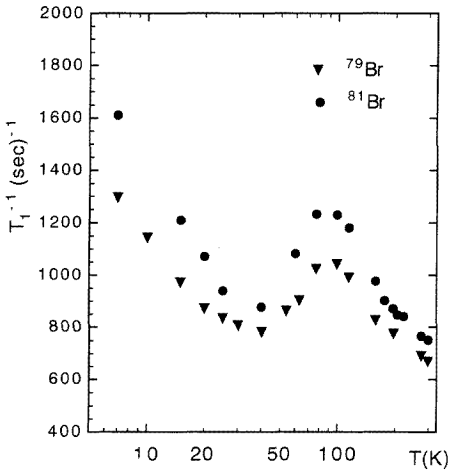

Figure 2. Measured ^{79}Br and ^{81}Br relaxation rate data as functions of temperature.

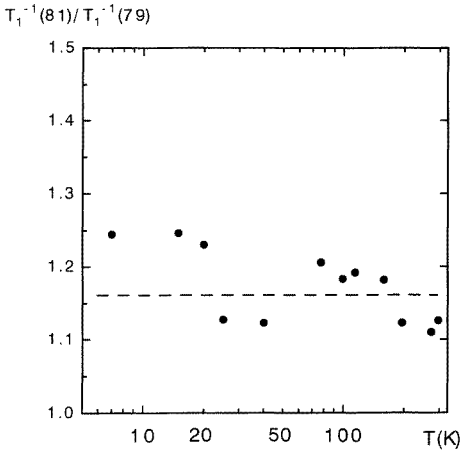

Figure 3. Ratio $T_1^{-1}(^{81}\mathrm{Br})/T_1^{-1}(^{79}\mathrm{Br})$ of relaxation rates, as a function of temperature. The broken line represents the expected value for a magnetic-dipole-dominated process, namely 1.16.

have the same crystal structure and both the Cl and the Br nuclei have spin 3/2. We also see that, for both compounds, T_1^{-1} increases as the temperature decreases at the lowest temperatures, in contrast with normal behaviour. The likely origin of both these effects is the splitting of the electronic ground state by the CEF. The energies of the ground-state multiplet are shown in figure 4 (Schmid *et al* 1987). Note that the splittings are quite different for the two compounds. The energies of the first and third CEF excited states, both with null magnetic moment, are 17 K and 138 K for $PrBr_3$ and 46 K and 198 K for $PrCl_3$. The changes in the populations of the levels of the multiplet over the range of temperatures studied will be significant and must be reflected in the spin–lattice relaxation process.

To evaluate relaxation rates we cannot say *a priori* that $(\omega_q \tau_\mu)^2 \ll 1$; however, if this inequality holds, equation (9) applies and T_1^{-1} is proportional to the correlation time τ_μ

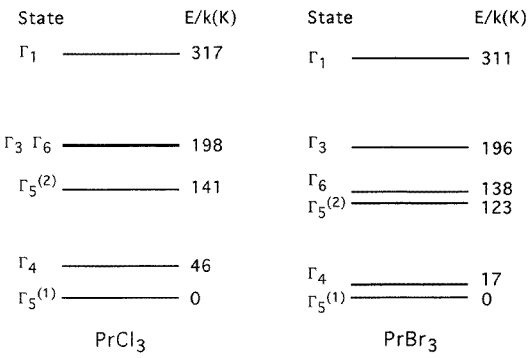

Figure 4. CEF energy level splittings for the ground-state multiplet of Pr^{3+} electronic configuration in $PrCl_3$ and $PrBr_3$.

and the geometrical factor A^2 defined in the previous section. This latter factor can be calculated using the known geometrical parameters (Schmid *et al* 1987). Estimated values of A^2 are presented in table 1. Values of the matrix element $\langle\Gamma_\mu|S_0|\Gamma_\mu\rangle$ are calculated using the known CEF eigenstates (Schmid *et al* 1987); results for states $\Gamma_5^{(1)}$ and $\Gamma_5^{(2)}$ are listed in table 1. We are now able to estimate the order of magnitude of the electron-spin correlation times from the experimental T_1^{-1}-values as about 10^{-10} s. Since $\omega_q \approx 10^7$ s^{-1}, the fast motion limit, $(\omega_q\tau_\mu)^2 \ll 1$, is a valid approximation and equation (9) applies. Assuming that the correlation between electrons corresponding to different Pr sites is negligible, the contribution of electrons from different sites is additive. Therefore, substituting the electronic populations $\rho_\mu = Z^{-1}\exp(-E_\mu/kT)$ with the partition function Z given by $Z = \sum_\mu \exp(-E_\mu/kT)$, and E_μ the electronic energy eigenvalues in equation (9), yields

$$T_1^{-1} = \frac{A^2}{Z}\sum_\mu \exp\left(\frac{-E_\mu}{kT}\right)|\langle\Gamma_\mu|S_0|\Gamma_\mu\rangle|^2\tau_\mu. \tag{11}$$

This equation explicitly shows the effect of populating the excited states.

Table 1. Calculated values of the matrix elements $|\langle\Gamma_\mu|S_0|\Gamma_\mu\rangle|$ and the geometrical parameter A^2 for $PrCl_3$ and $PrBr_3$.

	A^2 (10^{-12} s^{-2})	$\lvert\langle\Gamma_5^{(1)}\lvert S_0\rvert\Gamma_5^{(1)}\rangle\rvert$	$\lvert\langle\Gamma_5^{(2)}\lvert S_0\Gamma_5^{(2)}\rangle\rvert$	$\lvert\langle\Gamma_6\lvert S_0\rvert\Gamma_6\rangle\rvert$
^{35}Cl	2.24	0.71	2.71	1.0
^{79}Br	10.0	0.98	2.98	1.0
^{81}Br	11.6	0.98	2.98	1.0

Using the least-squares method, equation (11) was fitted to the $PrCl_3$ data. Initially the three lowest-temperature data points were fitted assuming that the contribution of the ground paramagnetic electronic state dominated the relaxation, and that the electron-spin correlation time was a constant. The result is the broken curve shown in figure 5. It gives ample evidence of the importance of the ground-state depopulation in accounting for the observed anomalous chlorine nuclear relaxation. However, the broken curve does not provide an adequate fit to the data. As a next step, a temperature-dependent term is added to the expression for the electron-spin correlation time as suggested by equation (10). The

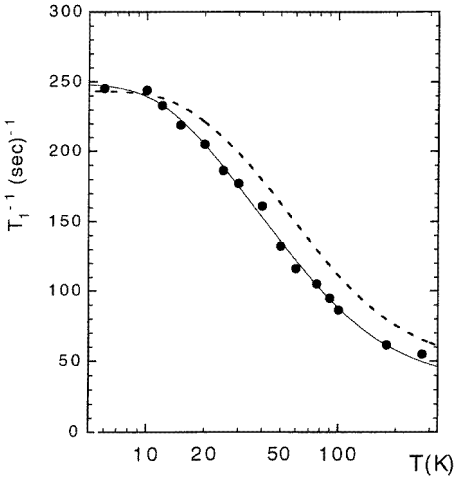

Figure 5. ^{35}Cl relaxation rate in $PrCl_3$. The lines are least-squares fits of equation (11). The broken curve shows the effect of the depopulation of the ground paramagnetic level $\Gamma_5^{(1)}$ assuming a temperature-independent electron-spin correlation time. The solid curve includes the added contribution of a temperature-dependent electron-spin correlation time.

result is the solid curve shown in figure 5; it provides an excellent fit to the data. There is no need to add further terms and, in particular, a term to represent the contribution of the first paramagnetic excited state $\Gamma_5^{(2)}$. This is somewhat surprising as this level will have a significant population above 100 K. On the other hand, only two data points were acquired above 100 K.

The three parameters obtained from the fit are given in table 2. The energy gap $\Delta/k = 26 \pm 5$ K has no easy interpretation. Indeed, given the energy level distribution (figure 4), the electron-spin correlation time cannot be explained by an Orbach process (Pake and Estle 1973, Mizuno *et al* 1991). Moreover, the functional form employed for the temperature dependence of the electron-spin correlation function is not unique. For example, a linear form gives an equally good fit to the data. What is clear is that the correlation time must decrease with increasing temperature in order to account for the data. Figure 6 shows the temperature variation in $\tau_5^{(1)}$ as deduced from the parameters in table 2.

Table 2. Electron-spin correlation times and energy gap parameters for $PrCl_3$ and $PrBr_3$.

	CEF state	τ_S (10^{10} s)	$T_{\mu 0}$ (10^{10} s)	Δ_μ/k (K)
$PrCl_3$	$\Gamma_5^{(1)}$	4.19 ± 0.08	11.0 ± 0.1	26 ± 5
$PrBr_3$	$\Gamma_5^{(1)}$	1.43 ± 0.08	2.0 ± 0.5	84 ± 16
	$\Gamma_5^{(2)}$	1.43 ± 0.08	3.1 ± 0.3	220 ± 40

The $PrBr_3$ data cannot be fitted in an equivalent fashion. This is obvious from a comparison of figures 1 and 2. In order to account for the secondary maximum occurring at about 90 K it is necessary to add a contribution from the paramagnetic $\Gamma_5^{(2)}$ state as described by two additional parameters T_{20} and $\Delta_5^{(2)}$. The data for both isotopes were fitted simultaneously. The resulting fits provide excellent representations of the data, as shown

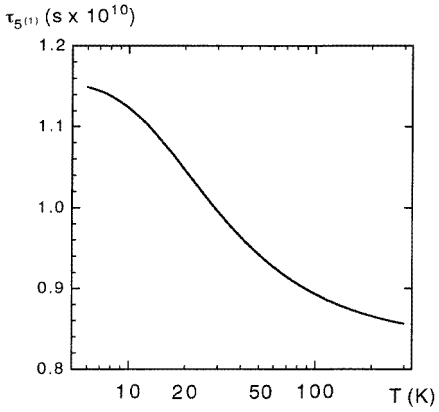

Figure 6. Calculated temperature dependence of the electron-spin correlation time for $PrCl_3$.

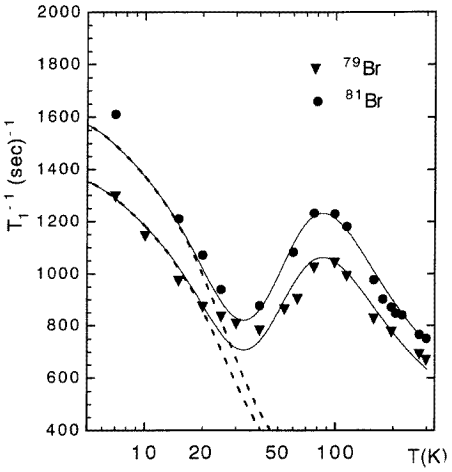

Figure 7. ^{79}Br and ^{81}Br relaxation rate in $PrBr_3$. The lines are simultaneous least-squares fits of equation (11). The broken curves account for only the depopulation of the ground paramagnetic level $\Gamma_5^{(1)}$. The solid curves include the additional contribution of the first excited paramagnetic level $\Gamma_5^{(2)}$.

by the solid curves in figure 7; the parameters are listed in table 2. The broken curves are the result of using only the ground paramagnetic state as was shown to be sufficient to fit the $PrCl_3$ data.

Because of the significant difference in the energies of the first excited states of the two compounds, the paramagnetic ground state of $PrBr_3$ will depopulate much more quickly as the temperature is raised than will the ground state of $PrCl_3$. As a consequence we would expect the paramagnetic $\Gamma_5^{(2)}$ level to become important at lower temperatures for $PrBr_3$ than for $PrCl_3$. This is what the data show, and this is what the analysis confirms. However, beyond this qualitative conclusion, the quantitative differences in the behaviour of T_1^{-1} for $PrCl_3$ compared with $PrBr_3$ must be due to differences in the details of the electronic structures and electron-spin dynamics of the two compounds. These differences cannot be articulated from the present experimental study.

5. Conclusion

The relaxation rates of the halogen nuclei in $PrCl_3$ and $PrBr_3$ in the temperature range 7–297 K are dominated by the magnetic dipole interactions between the halogen nuclei and the Pr^{3+} paramagnetic ions. The anomalous temperature dependence is a direct consequence of the CEF splitting of the ground-state multiplet of the Pr^{3+} configuration. The observed increase in T_1^{-1} at the lowest temperatures for both compounds is in large part due to the depopulation of the paramagnetic ground state of the multiplet; however, there is a significant contribution from the temperature dependence of the electron-spin correlation time. The dramatic difference between the behaviours of T_1^{-1} for the two compounds reflects the difference in CEF splittings. The occurrence of a secondary maximum in the relaxation rate of $PrBr_3$ is driven by the more rapid depopulation of its ground state and the subsequent enhanced importance of the contribution of the first excited paramagnetic level.

References

Abragam A 1961 *The Principles of Nuclear Magnetism* (Oxford: Clarendon)
Birkeland A and Svare I 1978 *Phys. Scr.* **18** 154
Bloembergen N 1957 *J. Chem. Phys.* **27** 572, 595
Bloembergen N and Morgan L O 1961 *J. Chem. Phys.* **34** 842
Bovet J M and Sharp R 1993 *J. Chem. Phys.* **99** 18
Colwell J H, Mangum B W and Utton D B 1969 *Phys. Rev.* **181** 842
Goovaerts E, De Readt D and Schoemaker D 1984 *Phys. Rev. Lett.* **52** 1649
Harrison J P, Hessler J P and Taylor D R 1976 *Phys. Rev.* B **14** 2979
Mizuno M, Asaji T, Nakamura D and Horiuchi K 1990 *Z. Naturf.* a **45** 527
Mizuno M, Asaji T, Tachikawa A and Nakamura D 1991 *Z. Naturf.* a **46** 1103
Morra R M, Armstrong R L and Taylor D R 1983 *Phys. Rev. Lett.* **51** 809
Pake G E and Estle T L 1973 *The Physical Principles of Electron Paramagnetic Resonance* (London: Benjamin)
Rager H 1981 *Z. Naturf.* a **36** 637
——1984 *Z. Naturf.* a **39** 111
Schmid B, Haig B, Furrer A, Urland W and Kremer R 1987 *J. Appl. Phys.* **61** 3426
Sharp R 1990 *J. Chem. Phys.* **93** 6921
——1992 *J. Magn. Reson.* **100** 491
——1993 *J. Chem. Phys.* **98** 912, 6092
Solomon I 1955 *Phys. Rev.* **99** 559
Su S and Armstrong R L 1993 *J. Magn. Reson.* A **101** 265
Su S, Armstrong R L, Wei W and Donaberger R 1991 *Phys. Rev.* B **43** 7565